

# Spurious Suppression Effect by Transmit Bandpass Filters with HTS Dual-Mode Resonators for 5 GHz Band

Kazunori YAMANAKA<sup>†a)</sup>, Member, Kazuaki KURIHARA<sup>†</sup>, Nonmember, Akihiko AKASEGAWA<sup>†</sup>, Masatoshi ISHII<sup>†</sup>, Members, and Teru NAKANISHI<sup>†</sup>, Nonmember

**SUMMARY** We report on the spurious suppression effect in low-microwave power transmitters by high temperature superconducting (HTS) bandpass filters (BPFs) which are promising for devices requiring BPFs with high-frequency selectivity. Some of the major issues on the power BPFs with HTS planar circuits for wireless communication applications are reviewed. As a case study for the HTS filter and its spurious suppression effect, this paper describes an example of the measured power spectrum density (PSD) on the suppression effect by one of our developed power BPFs with YBCO films for the 5 GHz band. It was designed with equivalent cascade resonators of 16 poles. We demonstrated the effect by HTS power filter in a power amplifier for the 5 GHz band.

**key words:** superconducting filter, spurious suppression, YBCO, power, transmit

## 1. Introduction

In recent years, it has become important to use efficient frequency resources of radio waves because demands of wireless communications have been increasing [1]. For example, mobile subscribers of the wireless communications are increasing, and then it is predicted that in the future many wireless communication systems will have a broader frequency band. In addition, channels of broadcasting systems will be increasing. Wireless communications tends to use radio waves with less frequency bands than the low microwave band because generally the waves provide better surface electromagnetic (EM) propagations than that of the higher frequency [2]. On the other hand, interexchange data via air between wireless communication systems tends to be increasing worldwide [3]. It means that efficient uses of the frequency resources and/or uses of the higher frequency band will be required. The issues including the above and other required issues, that is, the mobility as communicating, the reachable communication distance, the frequency resources, EM interferences between the systems and so on will have to be compromised [4]–[6]. Therefore, many kinds of advanced technology on improving usage of the frequency resources have been proposed, researched, and developed.

It is well known that high quality (with strong c-axis crystal orientation, small angle grain boundaries, etc.) HTS epitaxial films of YBCO (main component:  $\text{YBa}_2\text{Cu}_3\text{O}_{7-x}$ ,

$x = 0-0.5$ ) material, etc. can show surface resistance  $R_S$  values of 2–3 orders less than that of copper materials as a good electrical normal conductor in the low microwave band [7]. Making use of the HTS  $R_S$  property, HTS filters with EM resonators for low microwave band can show higher unloaded quality-factor ( $Q_U$ ) values, compared with filters with the same geometric structure and normal conductors. In cases of planar type filter circuits, HTS resonators with high quality YBCO films as the resonator part conductors can increase the ratio of the  $Q_U$  nearly as increasing the inverse ratio of the  $R_S$ . The high  $Q_U$  property is effective to constitute cascaded HTS EM resonators as for obtaining the higher frequency selectivity characteristics [8].

The HTS filter technologies are expected to be candidate technologies for efficiency uses of the frequency resources, because of the potential for frequency suppressing EM interferences between radio transceiver base stations and the adjacent channels. HTS receive (Rx) filter techniques for the low microwave band have already showed high selectivity characteristics comparable with those of concrete device design and fabrication processes [8]–[10] used in practical applications. On the other hand, transmit (Tx) filters for the low microwave radio band as a useful radio frequency (RF) region are operated at higher handling RF power value in the range of about 20–170 dB (these values depend on the airlink design of each radio system) as compared with that of the Rx filters [6]. HTS Tx filters for the same applications will require the similar handling power. For this reason, we need to consider HTS Tx filters as HTS power filters. HTS Tx filter developments are more difficult, because of the issues on RF power, compared to that of HTS Rx filters. In recent years, our previous R&Ds for the power filters around 5 GHz band have been reported [11]–[14].

In this paper, we describe R&D major issues on the HTS filters in order to handle the higher power, and address some promising applications for the HTS power filters. Next, we report on our experimental result of the spurious suppression effect by an HTS power filter in a radio transmit system that provides a transmitter with a RF power amplifier for 5 GHz band and broadband for the future wireless communications.

## 2. Issues on HTS Power Filters for RF Tx

In this section, issues for conventional RF transmitters

Manuscript received September 5, 2008.

Manuscript revised November 17, 2008.

<sup>†</sup>The authors are with Fujitsu Limited & Fujitsu Laboratories Ltd., Atsugi-shi, 243-0197 Japan.

a) E-mail: yamanaka-kaz@jp.fujitsu.com

DOI: 10.1587/transele.E92.C.288

for wireless communications for the low microwave band, broad bandwidth, and moderate Tx output handling maximum power from 20 to over 40 dBm are summarized. In addition, the issues to be solved and the effect are addressed when HTS filters are adapted to the transmitters.

## 2.1 RF Transmitter

An RF transmitter for a wireless communication system with a digital modulation/demodulation method for the low microwave band is considered hereinafter. When the modulated RF signal is inputted to an RF power-amplifier (PA) of the final stage, the output signal of the PA generally increases the spectral sidelobe regrowth as increasing the input signal power. The above modulations provides time-varying amplitude characteristics of the modulation wave envelope such as simple quadrature amplitude modulation (QAM), multilevel QAM modulation, multi-carrier modulations including the orthogonal frequency division multiplexing (OFDM) method, and the code division multiplexing (CDM) method [4].

On wireless communications, the regrowth problem has a possibility to give other radio receivers interferences due to the adjacent leakage power (ACP) when the wireless communication channels in the adjacent frequencies are assigned, and there is the radio which can receive in the coverage of the transmit EM wave [5]. Various kinds of techniques have been proposed and utilized in order to improve the problem. One of the typical methods for the regrowth suppressing is to improve the I/O linearity in the required power range of the PA under large backoff operation of it with larger output power capability than the required capability. In addition, distortion compensation techniques for the PA have been known [15]–[18]. The major compensation techniques are grouped into different types such as pre-distortion, feed-forward, and feed-back methods. There can be methods to combine them. In addition, not only analog but also digital method in the pre-distortion type have been developed in the PAs for the low microwave frequency applications in recent years since digital circuit techniques (for example, ADC circuit) have been developed with higher speed and larger scale. These methods have advantages and disadvantages. As requiring the larger quantity of the compensation, the wider frequency band, the higher frequency, and power consumption efficiency, the compensations tend to become more difficult in many cases.

Figure 1 shows a model block diagram by the conventional methods for the spurious suppression (in the following, “spurious” will be used in the same meaning as “unwanted” in the out-of-band and spurious domains by the recent regulation.), where RF-PA means RF power amplifier in wireless-communication base stations. On the other hand, the interferences by the Tx system spurious spectrum for the broader band communications to the ACP will be suppressed using a high selective filter on the RF-PA output side [5]. This idea is simple in appearance. However, these microwave power filters that are satisfied with the practical

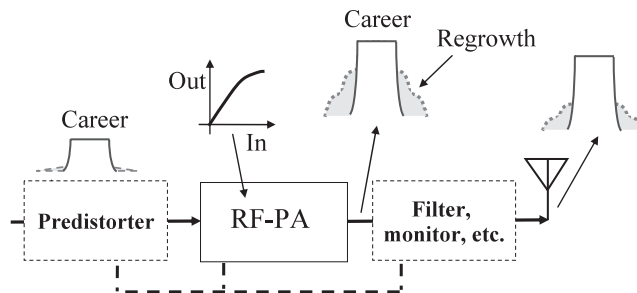


Fig. 1 A model block diagram by one of the conventional methods [19].

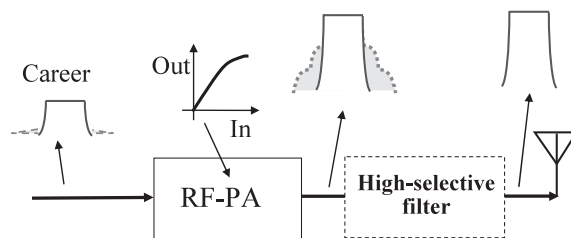


Fig. 2 A model block diagram by a method using a high-selective bandpass filter [19].

requirements have R&D issues in many cases. The HTS power filters R&Ds have the possibility for the application of the ACP suppression. The high-selective HTS power filters with both the lower spurious-spectrum and the lower energy-loss will be expected for the application. Figure 2 shows a model block diagram by a method using a high-selective bandpass filter (BPF).

## 2.2 $Q_U$ and HTS Material [20]

3-dimensional waveguide and planar circuits as microwave BPF structures using electromagnetic (EM) resonators are well known. If the EM resonators are made of the same materials at the same resonant frequency and operating temperature, the waveguide circuit resonator can have higher  $Q_U$  value and handling power than that of the planar circuit resonator generally known. Therefore, high-quality superconducting materials as the resonator conductor part can be considered effective to obtain higher  $Q_U$  than that using only normal conductor like copper or silver materials. Furthermore, in the low microwave band, the HTS planar circuit resonator that is made by using high-quality epitaxial HTS films with the lower  $R_S$  value can provide more compact size and higher  $Q_U$  than that of the normal metal waveguide in the case of the same frequency. As obtaining higher frequency selectivity by constituting the optimized filter circuits using the higher  $Q_U$  resonators with each other, the filter can have lower transmission energy loss.

The relation between each Q factor in the planar circuit filter with the EM resonators is given by

$$Q_U^{-1} = Q_C^{-1} + Q_D^{-1} + Q_R^{-1} + Q_{other}^{-1}, \quad (1)$$

where  $Q_C, Q_D, Q_R, Q_{other}$  are the conductor Q, the substrate

dielectric  $Q$ , the radiation  $Q$ , and the other part  $Q$ , respectively.  $Q_{other}$  consists of contributions from the interconnects, the package and so on. The planar circuits for RF applications are usually packaged into metal conductor containers to shield the external EM fields. In this case,  $Q_R$  can be regarded as positive infinity value due to no radiation loss as we consider that the filter circuit is included the package. The expression (1) means that  $Q_C$  has higher value as decreasing the  $R_S$  of HTS materials that are used in the circuits. That is, obtaining HTS materials with the lower  $R_S$  for the high  $Q$  resonator applications is important. Planar type circuits of the HTS Tx filters are candidates for the applications with moderate RF power (around 30–40 dBm) and low microwave band (around UHF-6 GHz band). In the HTS planar circuits like microstrip type, it is important to deposit lower  $R_S$  HTS films on both sides of the substrates with very low dielectric loss corresponding to very high  $Q_D$ .

In our previous R&D [9], [10], YBCO films were deposited on both sides of the MgO(100) substrate, which has a  $Q_D^{-1}$  on the order of  $10^{-6}$ . Depositions were carried out under various deposit conditions. The YBCO films with the substrates were patterned using photolithography to make resonator samples with hairpin microstrip lines for the 2 GHz band. The measured  $Q_U$  values of the 2 GHz-band YBCO microstrip-line resonators with different film-quality and normalized-thickness under a small signal input condition are shown in Fig. 3 [10], where  $t$  is the film thickness, and  $\lambda_L$  is London penetration length. The film characterization and analyses were carried out [9]. The results are summarized as follows.

All of the H and L type films showed strong c-axis orientation normal to the substrate as the X-ray diffraction (XRD)  $\theta - 2\theta$  easurement results. However, the XRD  $\phi$  scan measurement results showed main diffracted peaks corresponding to 90 degree between the grain boundary angles for the H films, and corresponding to 45 degree for the L films, respectively. In addition, the H films generally observed higher dense microstructures and fewer phase segregations than that of the L films by transmission electron microscopy. The relations between  $R_S$ ,  $Q_U$ ,  $t$ ,  $\lambda_L$  and the resonator device geometric and material parameters for EM calculations can be calculated theoretically and approximately using a conventional superconducting electromagnetism method. The comparative two curves with measured points in Fig. 3 were calculated by the method.

The power dependences of the resonant frequency for the 2 GHz band resonators were examined [9] to clarify the power dependence of the same YBCO films. Each resonator's resonant frequency shifted gradually as increasing the transmitted power. Figure 4 shows that each normalized resonant frequency shift of the H films were less than that of the L films at the same applied power [9]. Here,  $Max H_{RF}$  means evaluated maximum RF magnetic field in each YBCO resonator circuit by numerical calculations corresponding to the input power, given by

$$Max H_{RF} = k_g P_{in}^{1/2}, \quad (2)$$

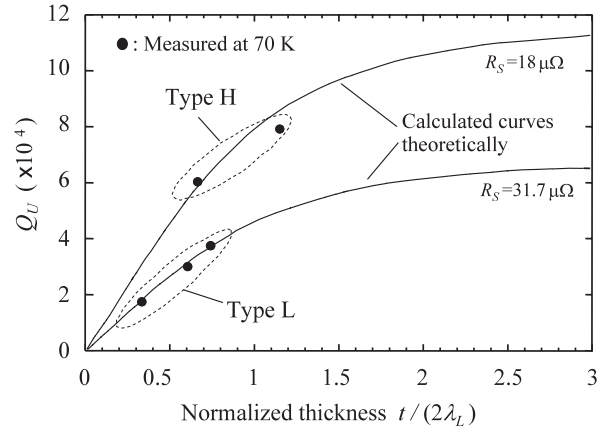


Fig. 3 Measured  $Q_U$  values (solid dots) of 2 GHz-band YBCO microstrip-line resonators with different film-quality and normalized-thickness under small signal input condition [10].

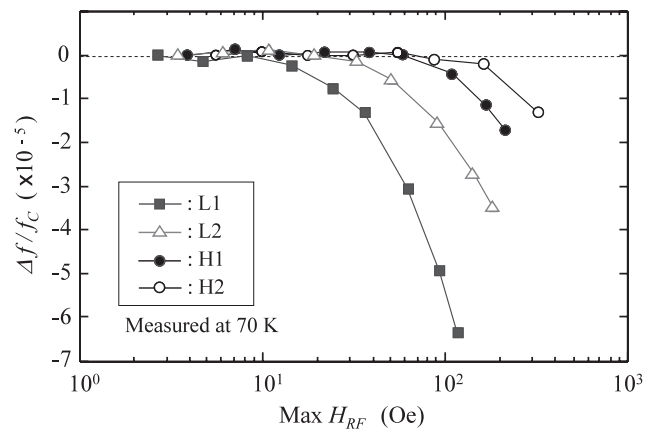


Fig. 4 Measured resonant shift  $\Delta f/f_c$  versus evaluated maximum RF magnetic field for 2 GHz-band YBCO MSL resonators with different film quality [9].

where  $P_{in}$  is the input power (W),  $k_g$  is a coefficient decided by the geometric structure and materials of the resonator device.  $\Delta f/f_c$  is the resonant frequency shift normalized by resonant frequency  $f_c$  as no  $Max H_{RF}$  assumption.

For many RF power applications, the H type film quality is better as compared with the L films. This shift can be understood that a superconducting RF resonator shows the resonant frequency shift by the applied power as a superconducting material has the magnetic penetration depth change caused by like artificial weak links, micro-impurities, defects, angle grain boundaries, which behave like weak links in YBCO materials [21]–[24]. The reason is suggested that inductive reactance in the equivalent circuit of the resonator is changed because the kinetic inductance is changed by RF magnetic field that occurred by the applied input power. To summarize, we found experimentally that the film quality and film thickness are important characteristics for microwave high-Q power applications.

### 2.3 Cryo Packaging

In wireless applications with HTS planar circuits, a packaging method in a system is explained as follows: The cold head of a cryocooler is covered with a vacuum chamber. HTS filters, of which HTS circuit substrates are packaged metal containers with RF connectors, are mounted on the cold head. The RF connectors are connected with coaxial cables to the hermetic RF connectors on the chamber. Obviously, this method can be changed by the cryostat design differences. In the packaging and mounting, there are the following technical issues [25]:

- (a) To relax thermal stress between room temperature (RT) and the operating cryogenic temperatures (OCT),
- (b) To suppress heat transfer from the outer of the chamber at RT and the filters at the OCT,
- (c) To minimize the joule heating in the HTS devices and/or other cryo-devices,
- (d) To decrease the heat capacity,
- (e) To minimize the joule heating in the RF cables as the RF input power increases.

Furthermore, (b) and (c), and (e) surfaces obviously in the RF power applications due to the larger RF input power into the chamber, RF cables, and HTS filter than those of only the Rx.

It is desired that these issues should be improved as much as possible, when the technologies are applied to the cryostat. (a) is important to prevent the devices from the deterioration by the cryostat power on-off operation cycle. Also (b), (c), (d), and (e) improvements will give lower thermal load of the cryocooler, thereby the smaller cryostat will be obtained.

### 2.4 TM-Mode Disk Patch Filter

R&Ds on HTS power filters have been reported [11]–[14], [20]–[36]. Gradually those characteristics have improved for the applications. In the HTS planer circuits with microstrip structure, TM-mode HTS disk-patch resonators are effective to improve the power handling capability as compared with HTS resonators with the narrow-line shaped patterns [20], because the HTS disk-patch patterns can provide lower current density on the pattern surface than that of the narrow one at the same transmitted-power, resonant-frequency, and I/O couplings. For this reason, the disk patch resonator is a kind of candidate structures of the HTS power filters. Figure 5 shows a simplified drawn model of TM-mode HTS disk patch resonator, where the HTS ground surface was contacted to the normal metal electrode layer on the bottom of the metal package. Each signal pin and outer conductor of the I/O RF coaxial connectors (SMA type) was connected electrically to each electrode for the I/O and the metal package, respectively. In the TM-mode HTS disk patch resonators as shown in Fig. 5, the power handling capability in the different TM modes were compared by numerical EM simulations, etc. at the same conditions on the

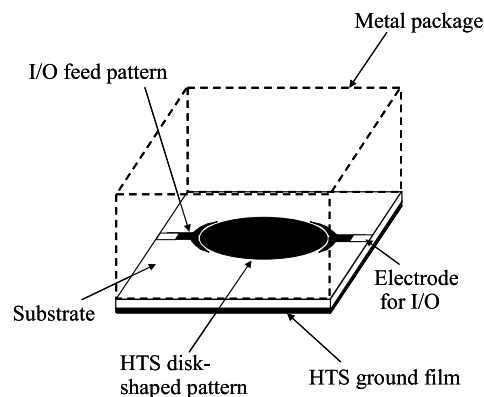


**Fig. 5** A model of TM-mode HTS disk patch resonator (RF connectors, etc. abbreviated). Dashed lines show the inner walls of the metal package.

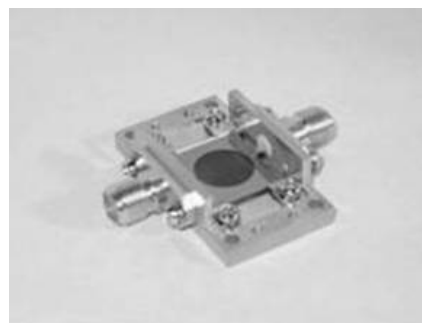


**Fig. 6** A photograph of a  $TM_{11}$  mode resonator sample with YBCO film/LAO crystal substrate/YBCO film layers for 4 GHz band, the top package cover removed [36].

resonant frequency, geometric structure, and materials [14]. These resonators with the different modes made the size adjustments for obtaining the same resonant frequency each other. The simulation results around 5 GHz on the  $TM_{01}$  and  $TM_{11}$  cases showed that the power handling capability of the  $TM_{01}$  is larger than that of the  $TM_{11}$ .

On the other hand, the disk size of the  $TM_{01}$  is also larger than that of the  $TM_{11}$ . When the HTS power filters with compact size are needed, the  $TM_{11}$  mode resonators may be candidates. Actually, the experiments on the handling power of  $TM_{11}$  mode were carried out [29], [36]. Figure 6 shows a photograph of a  $TM_{11}$  mode resonator sample with YBCO film/LAO ( $LaAlO_3$ ) (100) crystal substrate/YBCO film layers for 4 GHz band, the top package cover removed [36]. As a result on the experiments up to about 40 dBm input, we clarified the conditions to obtain the 3rd Intermodulation distortion (IMD3) value less than  $-60$  dBc at the handling power 10 W (40 dBm) at 4 GHz band in the case using LAO (100) and MgO (100) crystal substrate, respectively [29], [36].

To obtain the optimized filtering characteristic that depends on the required specification corresponding to the application, multistage (or multi-section) filter are generally used. To have designed frequency responses along the specification, there is a need to adjust the EM coupling coeffi-

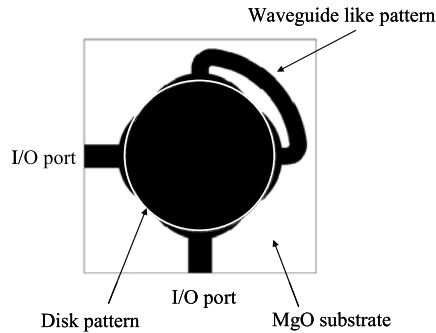


**Fig. 7** Top view of a model [11] of the  $TM_{11}$  dual-mode disk-patch resonator circuit patterns.

cients between the resonators. The range of each coefficient depends on the filter structure. On the other hand, to design a multistage HTS power BPF, each filter is compact size and has high power handling are required.

A dual mode resonator can reduce the size of a filter in half because it has two-resonance mode in one filter. We reported  $TM$  dual-mode disk-patch HTS resonators with novel patterns for dual-mode resonance [11], [12], [37]. These reported patterns have a circle disk shape to uniform the current density in the resonator disk. Figure 7 illustrates the pattern of the developed filter the  $TM_{11}$  dual mode disk-patch resonators [11]. It has a waveguide like pattern to generate a dual mode. The waveguide length is about  $\lambda/4$  of resonance frequency. The coupling coefficient of dual mode can be controlled with the waveguide length.

$TM$  dual-mode disk-patch resonator with HTS films using this perturbation method was designed with EM simulations. Strong  $c$ -axis orientated YBCO films on MgO (100) substrate were used. The sample was fabricated using lithography and etching techniques. The fabricated filter circuit was packaged in a gold-plated copper box. The IMD3 performance was measured using a two-tone method at temperature of 65 K. As the examination results, this filter has a very low IMD3 of  $-73$  dBc with an output power of 40 dBm. These values are enough for some practical wireless applications. The current density of the waveguide like pattern is not so significantly large was calculated by EM simulations (data not shown). It suggests that the waveguide pattern works a delay line not a part of a resonator. This filter has advantage for multistage filter, because it is possible to fabricate a dual mode filter with only one side patterning.

To develop multistage HTS BPFs with higher frequency selectivity, frequency responses of HTS BPF that consists of two-cascaded dual-mode resonators with YBCO films were simulated numerically by method of moment, etc. [13]. Also, BPFs with two-cascaded dual mode resonators with different height condition of the package inner ceiling were made. The results showed that spatial EM field and a transmission line for the coupling influenced the signal coupling between the dual-mode disks. The spatial EM field generated the coupling with and anti-resonance (attenuation response) between the resonators [13].

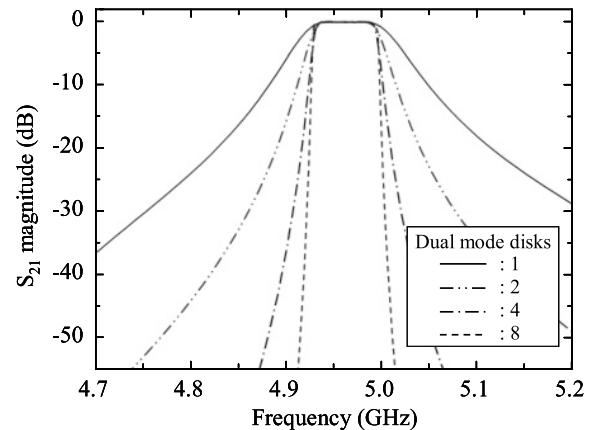


**Fig. 8** As simulation results, the disk total number dependence of  $S_{21}$  magnitude frequency response for BPFs cascaded the dual-mode disk patch resonators.

Next, we introduce circuit simulations on HTS BPFs that consist of cascaded dual-mode resonators extended up to 8 disks. The resonator was assumed to be with  $TM_{11}$  dual mode generated by the waveguide like method. The simulations in the part of each dual-mode resonator were carried out by method of moments. Assuming that signal between the resonators was coupled by transmission lines that were adjusted its electrical length and characteristic impedance, linear circuit simulations were done. That is, these resonators were not coupled by spatial EM fields. Figure 8 shows a summary of simulations in which the total disk number dependence of  $S_{21}$  magnitude as function of frequency for BPFs cascaded the dual-mode disk patch resonators. In Fig. 8, it was assumed that each disk diameter is 1 cm, substrate with thickness of 0.5 mm and specific dielectric constant of 9.7 as the simulation conditions. As the number of dual-mode disks were 8 (it means equivalent 16 single disks), the maximum slope showed about 30 dB/5 MHz.

On the base of the above results, BPF samples with 8 cascaded dual-mode disk resonators with YBCO films were made (mentioned at [26]). Figure 9 shows a photograph of a sample BPF with the 8 dual-mode disks with YBCO films on both sides of MgO (100) substrates. All of the YBCO films that were used for the sample device had strong  $c$ -axis orientation normal to the MgO substrate with thickness of 0.5 mm. Each YBCO films were patterned using photolithography method. The signal layer YBCO patterns on the substrate consisted of 4 disk-like shapes (the diameter of about 1 cm), microstrips and waveguide-like shapes for the I/O feeds and the coupling between the adjacent disks, and so on. Metal electrodes for the interconnections were deposited and patterned on the YBCO-patterned substrates [25]. The patterned substrates were cut using a dicing saw to mount those in a metal package. The sample device provided two patterned substrates. The patterned substrates each other interconnected with Indium solder and a metal ribbon on the package lower part. In addition, the EM cou-

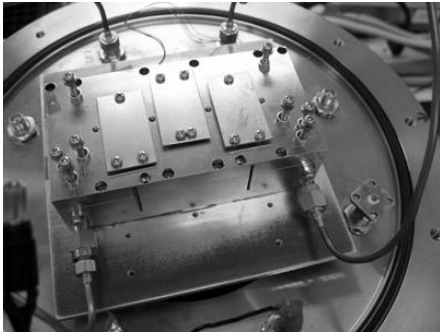


**Fig. 9** A photograph of a sample BPF with the 8 dual-mode disks with YBCO films, which shows the microwave measurement setup around the sample before cooling without the cryostat chamber cover.

pling adjusting mechanism was set in the package. The I/O feeder electrodes and coaxial connectors (SMA type) also interconnected with Indium solder. The sample BPF provided eight dual-mode disk-patch resonators with  $TM_{11}$  and YBCO films. The photograph of Fig. 9 also shows the microwave measurement setup around the sample before cooling examination. The top vacuum chamber of the cryostat was removed in Fig. 9. The sample provided screws to adjust the frequency response. The screws were for adjusting the coupling coefficients mainly. It is often important for each screw structure, position and materials (using conductors and/or dielectrics) to keep as fewer energy losses as possible.

**3. Spurious Suppression by HTS Power BPF**

Examinations to suppress spurious spectrum of broadband transmit signal through an RF-PA for 5 GHz band was carried out using HTS power filters. Here, we will show the examination using the BPF sample that was used with 8 dual-mode disk resonators mentioned above. A schematic diagram of the microwave power measurement for the examinations allowable up to about 40 dBm peak at the DUT input is illustrated in Fig. 10.

In the examination, the S.G. operation was programmed to generate modulation signal with a wider band than that of practical applications for the future applications of broadband wireless communications. The modulation method was used to extend the RF bandwidth of IEEE 802.16e as a kind of OFDM method. The RF bandwidth extended the original band to 75 MHz with the total subcarrier number of 1024. Table 1 shows the major modulation conditions to be used in the examinations.

Peak to average power ratio (PAPR) is important for the RF-PA. The peak power of a RF-PA needs to be within the dynamic range. In RF Tx systems with digital modulations, clipping the peak power causes the bit-error rate (BER) to increase. The PAPR value depends on kinds of modulated signal and the number of the sub-carriers. PAPR value of approximate 12 dB at the PAPR probability of  $10^{-3}$  in the IEEE 802.16e-2005 standard was estimated by Ref. [38]. Hence, in the case of OFDM modulation for the examination

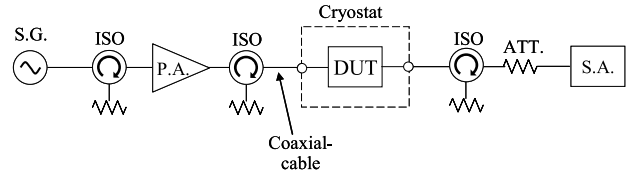


**Fig. 10** Schematic diagram of the microwave power measurement, where S.G.: RF signal generator with modulation function, P.A.: RF power amplifier, ISO: isolator with terminal load, DUT: device under the test (a sample HTS BPF), and S.A.: spectrum analyzer.

**Table 1** The major modulation conditions for the microwave power measurement.

Method	Extended IEEE 802.16e-2005
Primary modulation	16QAM
Code rate	1/2
Secondary modulation	OFDMA

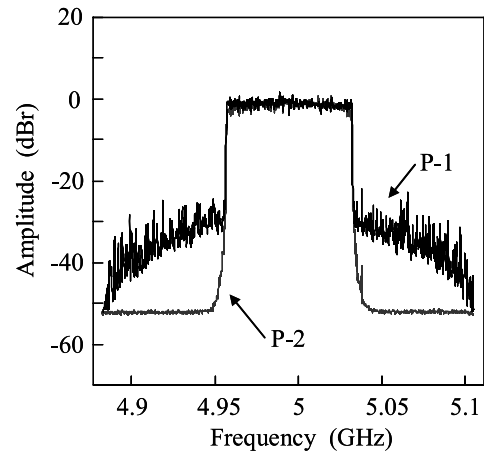


**Fig. 11** A PSD profile comparison of the examination results. P-1 and P-2 show the output-side PSD of the P.A. and the sample device, respectively.

in Table 1, the PAPR is considered larger than that of the standard. Figure 11 shows a power spectrum density (PSD) profile comparison of the examination results.

P-1 and P-2 show the output-side PSD of the P.A. and the sample device, respectively. Each spectrum shows an averaged profile of 30 spectra because of modulated signal varying as function of the time. The sample temperature was kept at 65 K. It was succeeded that the sample device suppressed enough the P-1 sidelobe spectrum that was regrown by the RF-PA nonlinearity.

**4. Conclusion**

In this paper, some of the major issues on the power BPFs with HTS planar circuits for wireless communication applications were reviewed. Furthermore, a spurious suppression effect by Tx BPFs with HTS dual-mode resonators for 5 GHz band was introduced.

To solve or improve the issues, we introduced some

of the methods as well as our R&D. This paper focused on (1) spectrum regrowth due to RF transmitter nonlinearity, (2)  $Q_U$  and HTS material quality, (3) cryo packaging, especially under the power handling, (4) TM mode disk patch resonators as some candidates for planar power HTS BPF structure.

On the base of the methods and results, HTS power BPFs with planar circuits were fabricated. As one of the BPFs, we showed schematically the BPF with eight dual-mode disk-patch resonators with  $TM_{11}$  and YBCO films. To suppress a spurious spectrum, which was regrown by a RF-P.A., using this HTS power BPF was demonstrated. To generate one of the widest band spectrum as an example of the broadband technique for the future wireless communications, the suppression effect examination was performed under the conditions to extend the bandwidth of a conventional modulation method.

### Acknowledgments

We would like to thank S. Futatsumori, Dr. T. Hikage, Prof. T. Nojima of Hokkaido University for assistance for the OFDM modulation extending. Furthermore, this work was supported in part by "Research and development of fundamental technologies for advanced radio frequency spectrum sharing in mobile communication systems" from the Ministry of Internal Affairs and Communications (MIC) of Japan. We would like to thank MIC for their support.

### References

- [1] H. Harada, M. Kuroda, H. Morikawa, H. Wakana, and F. Adachi, "The overview of the new generation mobile communication system and the role of software defined radio technology," *IEICE Trans. Commun.*, vol.E86-B, no.12, pp.3374–3384, Dec. 2003.
- [2] Q. Bi, G.I. Zysman, and H. Menkes, "Wireless mobile communications at the start of the 21st century," *IEEE Commun. Mag.*, vol.39, no.1, pp.110–116, Jan. 2001.
- [3] S. Takeuchi, "Recent trend in technologies developments for wireless communications," 2005 IEEE International Symposium on Microwave, Antenna, Propagation and EMC Technologies for Wireless Communications (MAPE 2005) Proceedings, vol.1, pp.1–7, Aug. 2005.
- [4] B. Razavi, *RF Microelectronics*, Prentice Hall (a Pearson Education Company), 1998.
- [5] N. Nakajima and T. Nojima, "Advanced RF technologies and future requirements for mobile communication base stations," *IEICE Trans. Electron.*, vol.E85-C, no.12, pp.1950–1958, Dec. 2002.
- [6] D.M. Pozar, *Microwave and RF Wireless Systems*, John Wiley & Sons, 2001.
- [7] A. Bourdillon and N.X. Tan Bourdillon, *High Temperature Superconductors, Processing and Science*, pp.269–273, Academic Press, 1993.
- [8] J.-S. Hong and M.J. Lancaster, *Microstrip Filters for RF/Microwave Applications*, John Wiley & Sons, 2001.
- [9] K. Yamanaka, A. Akasegawa, and T. Nakanishi, "Effect of YBCO film characteristics on RF properties of MSL resonators with these films," *Mat.Res.Soc. Symp. Proc.*, vol.659, II6.2.1–II6.2.6, 2001.
- [10] A. Akasegawa, K. Yamanaka, T. Nakanishi, and M. Kai, "High-temperature superconducting materials," *FUJITSU Sci. & Tech. J.*, vol.38, no.1, pp.31–38, June 2002.
- [11] M. Ishii, A. Akasegawa, T. Nakanishi, and K. Yamanaka, "Novel dual mode disk-shaped resonator filter with HTS thin film," *J. Phys.: Conf. Ser.* 97, 012149, 2008.
- [12] A. Akasegawa, T. Nakanishi, K. Yamanaka, and M. Ishii, "High-Tc superconducting dual-mode disk resonators with attenuation poles using ground-slot," *APMC 2007 Proceedings*, 2007.
- [13] K. Yamanaka, M. Ishii, A. Akasegawa, T. Nakanishi, J.D. Baniecki, and K. Kurihara, "5 GHz HTS power filters with TM-mode microstrip disk resonators," *Physica C*, vol.C468, pp.1950–1953, 2008.
- [14] K. Yamanaka, K. Kurihara, A. Akasegawa, and M. Kondo, "Design of a mechanical tuning for superconducting microwave power filters," *J. of Supercond. and Novel Mag.*, vol.20, no.1, pp.31–36, Jan. 2007.
- [15] T.H. Lee, *Planar Microwave Engineering*, Cambridge Univ. Press, 2004 etc.
- [16] S.W. Chung, J.W. Holloway, and J.L. Dawson, "Open-loop digital predistortion using cartesian feedback for adaptive RF power amplifier linearization," *IEEE MTT-S International Symposium*, pp.1449–1452, 2007.
- [17] T. Wang and J. Ilow, "Compensation of nonlinear distortions with memory effects in OFDM transmitters," *IEEE Globecom'04*, pp.2398–2403, 2004.
- [18] H.B. Nasr, S. Boumaiza, M. Helaoui, A. Ghazel, and F.M. Ghannouchi, "On the critical issues of DSP/FPGA mixed digital predistorter implementation," *IEEE APMC 2005 Proceedings*, vol.5, Dec. 2005.
- [19] K. Yamanaka, K. Kurihara, A. Akasegawa, S. Futatsumori, T. Hikage, and T. Nojima, "Spurious suppression effect by HTS power bandpass filters for 5 GHz band," *IEICE Technical Report*, SCE2008-13, MW2008-13(2008-4), 2008.
- [20] K. Yamanaka and K. Kurihara, "Superconducting filters for application to wireless-communication base stations," *IEICE Technical Report*, SCE2007-11, MW2007-11(2007-04), 2007.
- [21] D.E. Oates and A.C. Anderson, "Surface impedance measurements of  $YBa_2Cu_3O_{7-x}$  thin films in stripline resonators," *IEEE Trans. Magn.*, vol.27, no.2, pp.867–871, March 1991.
- [22] D.E. Oates, A.C. Anderson, D.M. Sheen, and S.M. Ali, "Stripline resonator measurements of  $Z_S$  versus  $H_{rf}$  in  $YBa_2Cu_3O_{7-x}$  thin films," *IEEE Trans. Microw. Theory Tech.*, vol.39, no.9, pp.1522–1529, 1991.
- [23] D.E. Oates, A.C. Anderson, and P.M. Mankiewich, "Measurement of the surface resistance of  $YBa_2Cu_3O_{7-x}$  thin films using stripline resonators," *J. Supercond.*, vol.3, pp.251–259, 1990.
- [24] S. Miura, K. Hashimoto, J.-G. Wen, K. Suzuki, and T. Morishita, "Electrical properties of  $YBa_2Cu_3O_x$  films grown by liquid phase epitaxy," *IEICE Trans. Electron.*, vol.E81-C, no.10, pp.1553–1556, Oct. 1998.
- [25] K. Yamanaka, A. Akasegawa, T. Nakanishi, and M. Kai, "YBCO film properties for 2 GHz band receivers with HTS filters and the filter characteristics," *Trans. of the MRS of Jpn.*, vol.29, no.4, pp.1279–1283, 2004.
- [26] K. Yamanaka, M. Ishii, K. Sato, A. Akasegawa, T. Nakanishi, and K. Kurihara, "Multistage of HTS power filters using dual-mode patch type resonators," *JSAP and related societies, Spr. Mtg. Extended abstracts*, 27p-NA-9/I, 2008.
- [27] G.-C. Liang, D. Zhang, C.-F. Shih, M.E. Johansson, and R.S. Withers, "High-power high-temperature superconducting microstrip filters for cellular base-station applications," *IEEE Trans. Appl. Supercond.*, vol.5, no.2, pp.2652–2655, June 1995.
- [28] B.A. Aminov, H. Piel, M.A. Hein, T. Kaiser, G. Müller, A. Baumfalk, H.J. Chaloupka, and S. Kolesov, "YBCO disk resonator filters operating at high power," *IEEE Trans. Appl. Supercond.*, vol.9, no.2, pp.4185–4188, June 1999.
- [29] K. Yamanaka, A. Akasegawa, M. Kai, and T. Nakanishi, "RF power dependence of microstrip disk resonators with YBCO films for 4 GHz band," *IEEE Trans. Appl. Supercond.*, vol.15, no.2, pp.1024–1027, June 2005.
- [30] T. Dahm, D.J. Scalapino, and B.A. Willemsen, "Microwave inter-

modulation of a superconducting disk resonator," *J. Appl. Phys.*, vol.86, pp.4055–4057, Oct. 1999.

- [31] A.P. Jenkins, K.S. Kale, D.J. Edwards, and D. Dew-Hughes, "Microstrip disk resonators for filters fabricated from TBCCO thin films," *IEEE Trans. Appl. Supercond.*, vol.7, no.2, pp.2793–2796, June 1997.
- [32] H. Higashino, A. Enokihara, and K. Setsune, "Recent progress in high- $T_c$  superconducting power filters," *Advances in Superconductivity IX (ISS'96)*, pp.1239–1244, 1996.
- [33] K. Setsune and A. Enokihara, "Elliptic-disc filters of high- $T_c$  superconducting films for power-handling capability over 100 W," *IEEE Trans. Appl. Supercond.*, vol.48, no.7, pp.1256–1264, July 2000.
- [34] A. Akasegawa, K. Yamanaka, T. Nakanishi, and M. Kai, "Power handling improvement by an upper conducting layer for 4 GHz-band HTS microstrip-disk filters with dual-mode," *Physica C*, vol.C445-448, pp.990–993, 2006.
- [35] K. Yamanaka, A. Akasegawa, M. Kai, and T. Nakanishi, "Intermodulation distortion characteristics of a 4 GHz-band HTS microstrip-disk filter," *Physica C*, vol.C445-448, pp.998–1002, 2006.
- [36] K. Yamanaka, A. Akasegawa, M. Kai, and T. Nakanishi, "RF power properties of YBCO-Film/LAO microstrip disk resonators for 4 GHz band," *IEICE Trans. Electron.*, vol.E89-C, no.2, pp.156–162, Feb. 2006.
- [37] A. Akasegawa, T. Nakanishi, K. Yamanaka, and M. Ishii, "Fabrication and estimation of a superconducting dual-mode disk resonator using ground-slot structure," *IEICE Technical Report*, SCE2007-8, MW2007-8(2007-4), April 2007.
- [38] S. Lloyd, "Challenges of mobile WiMAX RF transceivers," *IC-SICT'06*, pp.1821–1824, 2006.



**Kazunori Yamanaka** received the B.E. degree in Industrial Chemistry from Nihon University, Tokyo and M.S. degrees in Physics from Chiba University, Chiba, Japan in 1979 and 1981, respectively. He joined Fujitsu Laboratories Ltd., Japan in 1981, where he has been engaged in research and development of materials for superconducting devices, magnetic devices, and so on. He is a member of the Japan Society of Applied Physics, the Cryogenic Society of Japan, and the Institute of Electronics,

Information and Communication Engineers. Also, He is now with Fujitsu Limited and Fujitsu Laboratories Ltd.



**Kazuaki Kurihara** received the B.E. degree in Metallurgic Engineering and M.S. degree in Materials Science from Tokyo Institute of Technology, Tokyo, Japan in 1979 and 1981, respectively. He joined Fujitsu Laboratories Ltd., Japan in 1981, where he has been engaged in research and development of materials for ceramic materials and devices. He is a member of the Japan Society of Applied Physics and the Ceramic Society of Japan. Also, he is now with Fujitsu Limited and Fujitsu Laboratories Ltd.



**Akihiko Akasegawa** received the B.E. and M.E. degrees in Solid-state physics from Osaka University, Osaka, Japan in 1990 and 1992, respectively. He joined Fujitsu Laboratories Ltd., Japan in 1992, where he has been engaged in research and development of materials for superconducting devices. He is a member of the Japan Society of Applied Physics and the Cryogenic Society of Japan. Also, He is now with Fujitsu Limited and Fujitsu Laboratories Ltd.



**Masatoshi Ishii** received the B.E. and M.E. degrees in electrical engineering from Musashi Institute of Technology, Tokyo, Japan, in 1991 and 1993, respectively. In 1993, he joined Fujitsu Ltd., Kawasaki, Japan. In 1998, he joined Fujitsu Laboratories Ltd., Atsugi, Japan, where he has been engaged in research and development of dielectric and ferroelectric films for nonlinear optical devices and microwave devices. Mr. Ishii is a member of the Japan Society of Applied Physics. Also, he is now with Fujitsu

Limited and Fujitsu Laboratories Ltd.



**Teru Nakanishi** graduated from Hiratsuka Technical High School, Kanagawa, Japan, in 1986. He joined Fujitsu Laboratories Ltd., Atsugi, Japan in 1986, where he has been engaged in research and development of packaging materials for LSI circuits and superconducting devices. Also, He is now with Fujitsu Limited and Fujitsu Laboratories Ltd.